EBioMedicine 54 (2020) 102699

Contents lists available at ScienceDirect

EBioMedicine

journal homepage: www.elsevier.com/locate/ebiom

Research paper

Severe metabolic alterations in liver cancer lead to ERK pathway activation and drug resistance

Zeribe Chike Nwosu[a,*], Weronika Piorońska[a], Nadia Battello[b], Andreas David Zimmer[c], Bedair Dewidar[a,d], Mei Han[a], Sharon Pereira[e], Biljana Blagojevic[f], Darko Castven[e], Verodia Charlestin[g], Pavlo Holenya[f], Julia Lochead[f], Carolina De La Torre[h], Norbert Gretz[h], Peter Sajjakulnukit[i], Li Zhang[i], Matthew H. Ward[i], Jens U. Marquardt[e], Marina Pasca di Magliano[i], Costas A. Lyssiotis[i], Jonathan Sleeman[j,k], Stefan Wölfl[f], Matthias Philip Ebert[a], Christoph Meyer[a], Ute Hofmann[l], Steven Dooley[a,#]

[a] Department of Medicine II, Molecular Hepatology Section, Medical Faculty Mannheim, University of Heidelberg, 68167 Mannheim, Germany
[b] Luxembourg Science Center, L-4620 Differdange, Luxembourg, Luxembourg Centre for Systems Biomedicine, University of Luxembourg, L-4362 Esch-Belval, Luxembourg
[c] Signal Transduction Laboratory, Life Sciences Research Unit, University of Luxembourg, L-4367 Belvaux, Luxembourg
[d] Department of Pharmacology and Toxicology, Faculty of Pharmacy, Tanta University, 31527 Tanta, Egypt
[e] Department of Medicine I, Lichtenberg Research Group, Johannes Gutenberg University, Mainz, Germany
[f] Department of Biology, Institute of Pharmacy and Molecular Biotechnology, University of Heidelberg, 69120 Heidelberg, Germany
[g] Department of Chemistry and Biochemistry, University of Notre Dame, Notre Dame, 46556 IN, United States
[h] Medical Research Center, Medical Faculty of Mannheim, University of Heidelberg, Mannheim, Germany
[i] Rogel Cancer Center, University of Michigan, Ann Arbor 48109 MI, United States
[j] Medical Faculty Mannheim, ECAS TRIDOMUS-Gebäude Haus C, University of Heidelberg, 68167 Mannheim, Germany
[k] IBCS-BIP, Campus Nord, Karlsruhe Institute for Technology (KIT), 76021 Karlsruhe, Germany
[l] Dr. Margarete Fischer-Bosch Institute of Clinical Pharmacology and University of Tübingen, 70376 Stuttgart, Germany

ARTICLE INFO

Article History:
Received 21 November 2019
Revised 16 February 2020
Accepted 18 February 2020
Available online xxx

Keywords:
Metabolic state
Kinase inhibitors
Glutamine
Serine
Proliferation
Aerobic glycolysis
HCC

ABSTRACT

Background: The extracellular signal-regulated kinase (ERK) pathway regulates cell growth, and is hyper-activated and associated with drug resistance in hepatocellular carcinoma (HCC). Metabolic pathways are profoundly dysregulated in HCC. Whether an altered metabolic state is linked to activated ERK pathway and drug response in HCC is unaddressed.

Methods: We deprived HCC cells of glutamine to induce metabolic alterations and performed various assays, including metabolomics (with ^{13}C-glucose isotope tracing), microarray analysis, and cell proliferation assays. Glutamine-deprived cells were also treated with kinase inhibitors (*e.g.* Sorafenib, Erlotinib, U0126 amongst other MEK inhibitors). We performed bioinformatics analysis and stratification of HCC tumour microarrays to determine upregulated ERK gene signatures in patients.

Findings: In a subset of HCC cells, the withdrawal of glutamine triggers a severe metabolic alteration and ERK phosphorylation (pERK). This is accompanied by resistance to the anti-proliferative effect of kinase inhibitors, despite pERK inhibition. High intracellular serine is a consistent feature of an altered metabolic state and contributes to pERK induction and the kinase inhibitor resistance. Blocking the ERK pathway facilitates cell proliferation by reprogramming metabolism, notably enhancing aerobic glycolysis. We have identified 24 highly expressed ERK gene signatures that their combined expression strongly indicates a dysregulated metabolic gene network in human HCC tissues.

Interpretation: A severely compromised metabolism lead to ERK pathway induction, and primes some HCC cells to pro-survival phenotypes upon ERK pathway blockade. Our findings offer novel insights for understanding, predicting and overcoming drug resistance in liver cancer patients.

Fund: DFG, BMBF and Sino-German Cooperation Project

* Current Address of Corresponding author: Department of Molecular and Integrative Physiology, Rogel Cancer Centre, University of Michigan, Ann Arbor, 48109 MI, USA.
# Address of the Corresponding/Senior author: Department of Medicine II, Molecular Hepatology Section, Medical Faculty Mannheim, University of Heidelberg, 68167 Mannheim, Germany.
E-mail addresses: zcnwosu@umich.edu (Z.C. Nwosu), steven.dooley@medma.uni-heidelberg.de (S. Dooley).

https://doi.org/10.1016/j.ebiom.2020.102699

Research in context

Evidence before this study

Compared to healthy liver tissues, major components of metabolism such as metabolites and enzymes are abnormally expressed in liver cancer. It is also known that the RAS-RAF-MEK-ERK signalling pathway is hyperactivated in this cancer type, and that some inhibitors used in clinical cancer therapy act by blocking the ERK pathway. Treatment options for liver cancer are very limited, resistance to ERK pathway inhibitors is a known challenge, and factors that cause resistance to treatment are largely undefined. Whether liver cancer metabolic alteration is linked to the ERK signalling activation and drug response is unknown. In addition, whether the severity of metabolic alterations can predict tumours that will best respond to treatment is unexplored.

Added value of this study

We have demonstrated *in vitro* that severe metabolic alterations, ERK pathway activation, and the likelihood of drug resistance are interconnected in a crosstalk in which the metabolic derangement is ostensibly the initiating event. When metabolism is impaired, the ERK pathway becomes activated. Under this altered condition, treatment with ERK pathway inhibitors facilitate proliferation by inducing an increased metabolic activity, particularly glycolysis. We show that serine also accumulates, and can at least partially contribute to the pERK induction, although the mechanism is currently unclear. Using gene expression profile of human liver cancer tissues, we show that a high expression of ERK pathway components strongly correlate with the metabolic gene alterations often seen in liver tumour samples. We also presented 24 ERK gene signatures that could serve as a useful panel for predicting ERK pathway activation and the severity of HCC tumour metabolic changes.

Implications of all the available evidence

This study highlights the possibility that the inhibitors of ERK pathway induce contradictory effects in liver cancer, despite suppressing the pathway. Specifically, when liver cancer metabolism is fairly 'normal' or 'intact' (*e.g.* at the early stage of the disease) these inhibitors could be effective in preventing tumour progression. However, even though these inhibitors remain effective in blocking ERK pathway, when metabolism is severely compromised (*e.g.* at the advanced disease stage), the inhibitors can induce an undesired increase in metabolism, which favours tumourigenic activities. Therefore, tumour metabolic state at treatment and the specific effect of a treatment on tumour metabolism – even for compounds not designed to target metabolic pathways – may be an important factor to consider in future HCC treatment endeavours. Similarly, the combination of ERK pathway inhibitors with inhibitors of metabolism is an important research direction to be explored. Insights from this study also provide a rationale for exploring ways to include tumour metabolic features in the prediction of patients best suited for therapies that block the ERK pathway. Further studies are required to better explore metabolism-ERK signalling crosstalk in improving HCC patients' response to treatment.

αKG	alpha ketoglutarate
EGF	epidermal growth factor
ERK	extracellular signal-regulated kinase
GSEA	gene set enrichment analysis
HCC	hepatocellular carcinoma
MAPK	mitogen-activated protein kinase
MTT	3-(4,5-dimethylthiazol-2-yl)−2,5-diphenyltetrazolium bromide
RT-qPCR	reverse transcription quantitative polymerase chain reaction
SBP	serine biosynthesis pathway
TCA	tricarboxylic acid

1. Introduction

Epidemiological studies report a rising incidence of liver cancer and low patient survival rates [1,2]. There is an urgent need for effective therapies against liver cancer, of which >80% of cases are hepatocellular carcinoma (HCC). Kinase inhibitors (*e.g.* Sorafenib and Erlotinib) have been explored in the clinic for HCC therapy based on promising anti-cancer efficacy in preclinical studies. The majority of these inhibitors act by blocking the mitogen-activated protein kinase/extracellular signal-regulated kinase pathway (ERK pathway). This pathway is widely known to be upregulated in various cancer types and is considered a central driver of tumour progression. However, many patients who initially respond to therapies targeting the ERK pathway later develop drug resistance [3-5]. To date, the only first-line therapy against advanced HCC is the multi-kinase inhibitor Sorafenib, which extends survival by ~3 months. Similarly, Regorafenib, which was recently approved as a second-line therapy for patients whose tumour resisted Sorafenib also extends survival by ~3 months [6]. Clinical trials to improve the survival benefits of Sorafenib have been largely unsuccessful [7,8]. It is therefore important to understand the factors that contribute to poor response to therapy in order to better predict which patients will benefit from targeted therapies.

Metabolic alterations promote cancer cell survival and progression [9,10]. Human liver cancer harbours profound metabolic changes, notably the downregulation of genes associated with normal liver functions such as drug/xenobiotics metabolism and amino acid metabolism [11-15]. Whether the altered metabolic state affects HCC response to ERK pathway inhibitors is largely unaddressed. The poorly differentiated HCC cell lines are potentially useful models for studying how metabolism impacts therapeutic response. These cells largely retain human liver tumour metabolic gene expression pattern [15], and exhibit a dependency on extracellular glutamine (Gln) – a crucial amino acid in intermediary metabolism [16-23]. Therefore, in this study, we deprived HCC cells of extracellular Gln and examined the impact on metabolism, the ERK signalling pathway, and sensitivity to kinase inhibitors. Our findings show that severe alteration of HCC cell metabolism correlates with ERK pathway activation, and suggest that inhibiting the ERK pathway induces undesired consequences when metabolism is severely compromised.

2. Material and methods

2.1. Cell culture

The HCC cell lines HEP3B, PLC/PRF/5, HUH1, HEPG2, HLE, HLF and HUH7 were obtained from the Japanese Cancer Research Resources

Bank or American Type Culture Collection. SNU475 was a kind gift from Dr. Kathrin Woll (University of Heidelberg, Germany); SNU398 was from Dr. Francois Helle (University of Picardie Jules Verne, France), while SNU449 was from Dr. Cedric Coulouarn (INSERM, France). All cells were Mycoplasma-tested with PCR Mycoplasma Test Kit (PromoCell, Germany). HLE, HUH7 and SNU398 cells were re-authenticated by Short Tandem Repeat analysis. Liver cancer patient-derived cell lines (PDCLs) were established from surgical specimen obtained at the University of Mainz, Germany, following patient informed consent and local ethics committee approval. Isolation and establishment of PDCLs were as recently described [24]. The cell lines were cultured in DMEM (Lonza, BE12-709) supplemented with 2 mM glutamine, 10% foetal bovine serum (FBS), penicillin (100 μ/mL), streptomycin (100 μg/mL), and were used within 10 passages after thawing. For glutamine withdrawal experiments, the cells were washed 1x with Hank's Balanced Salt Solution (HBSS) or phosphate buffered saline (PBS) prior to experiments with glutamine-free media. Serine deprivation experiment were performed with culture media constituted with DMEM powder (D9802-1, USBiological) according to the manufacturer's instructions. The metabolites used for supplementation experiments as well as drugs/inhibitors used are listed in the Supplementary Table 3.

2.2. Proliferation and clonogenic assays

Cell proliferation was measured in quadruplicates using 3-(4,5-dimethylthiazol-2-yl)−2,5-diphenyltetrazolium bromide assay (MTT, M5655-1 G, Sigma) in 96-well plates. Most experiments comparing HUH7 and HLE cells were performed in parallel or on the same plate with HUH7 cells in the upper aspect of the plate and HLE cells in the lower aspect. Further details about the proliferation and clonogenic assays are in the Supplementary file.

2.3. Western blotting and quantitative PCR

Western blot, RNA isolation and quantitative reverse transcription PCR (RT-qPCR) were performed as recently described [15]. Antibodies used for western blot are as follows: AKT (rabbit, # 9272), pAKT (rabbit, # 9271) from Cell Signalling Technology; PSAT1 (rabbit, # PA5-22,124) from Thermofisher Scientific; and ERK (mouse, sc-135,900), pERK (mouse, sc-7383), goat anti-mouse IgG-HRP (sc-2060), and goat anti-rabbit IgG-HRP (sc-2301) from Santa Cruz Biotechnology. The gene primers used for qPCR are listed in the Supplementary Table 4.

2.4. Metabolomics profiling

For intracellular metabolite profiling of Gln-deprived HUH7 and HLE cells, the cells were seeded in triplicates in 12-well plates and cultured for 24 h with DMEM containing 10% dialysed FBS, 25 mM glucose and 4 mM Gln (Sigma-Aldrich). The same culture condition was used for glucose-carbon isotope tracing except that for the tracing experiment glucose-free DMEM was supplemented with 25 mM uniformly labelled glucose (U-^{13}C-glucose) (Cambridge Isotope Laboratories). The extraction of intracellular metabolites, quantification by gas chromatography-mass spectrometry (GC−MS) and mass isotopologue distribution analysis were performed as previously described [25]. For extracellular metabolite profiling in serum-free media, HLE and HUH7 cells were seeded in 12-well plates in duplicates. After overnight incubation, the culture media was changed to serum-free media (with or without Gln) to minimise any confounding effect of cell proliferation. 50 μl of media sample was collected from each of the duplicate wells at 0, 24, 28, 32, 48 h time points. Samples from each time point were pooled and subsequently analysed by GC−MS or liquid chromatography-mass spectrometry (LC-MS/MS) as previously described [26]. The metabolomics results were normalised to the corresponding cell count from parallel plate set-up. Further details on the metabolomics profiling of serine-free or -supplemented HLE cells are in the Supplementary file.

2.5. Microarray analysis of glutamine deprived HLE cells

Gene expression analysis of HLE cells cultured in complete media, Gln-free media and or in Gln-free media containing 20 μM U0126 was performed using Affymetrix human HuGene-2_0-st-type arrays. Biotinylated antisense cDNA was prepared according to the Affymetrix standard labelling protocol with the GeneChip® WT Plus Reagent Kit and the GeneChip® Hybridization, Wash and Stain Kit (Affymetrix, Santa Clara, USA). Afterwards, hybridisation on the chip was performed on a GeneChip Hybridization oven 640, followed by dye in the Fluidics Station 450 and scanning with GeneChip Scanner 3000. Custom CDF version 22 with ENTREZ-based gene definitions was used for array annotation [27]. Subsequently, the raw fluorescence intensity values were normalised by applying quantile normalisation and RMA background correction using SAS JMP10 Genomics package, version 6 (SAS Institute, North Carolina, USA). *Limma* package was used to identify differentially expressed genes. The microarray dataset has been deposited in the NCBI GEO under the accession number GSE123062.

2.6. Human HCC microarrays datasets

Five human HCC microarray datasets GSE14323 (19 non-tumour *vs* 38 HCC tissues), GSE25097 (243 non-tumour *vs* 268 HCC tissues), GSE14520 (220 non-tumour *vs* 225 HCC tissues), GSE39791 (72 non-tumour *vs* 72 HCC tissues) and GSE57951 (39 non-tumour *vs* 39 HCC tissues), altogether 593 non-tumour and 642 liver tumour samples, were obtained from the National Centre for Biotechnology Information Gene Expression Omnibus (NCBI GEO) and analysed as previously described [14]. A list of 458 genes associated with the RAS/RAF/MAPK/ERK pathway, including growth factors, were compiled from the KEGG database (https://www.genome.jp/kegg/) and published literature [3-5]. Using this list, the genes differentially expressed at $P<0.05$ in tumour *versus* non-tumour samples were extracted from the HCC datasets. Thereafter, the average log fold change of a differentially expressed gene across the datasets was used to rank and determine the upregulated or downregulated genes. Twenty four top upregulated ERK genes were selected and used for tumour stratification analysis.

2.7. HCC tumour stratification based on 24 ERK pathway gene signatures

The expression values for the 24 genes were extracted for each tumour sample in two HCC datasets − GSE14520 ($n = 225$ samples) and GSE25097 ($n = 268$ samples). Using these values, the tumour samples per dataset were ranked by their average expression of the ERK pathway genes and this along with *k*-means clustering was used to separate each dataset into highERK or lowERK group. After determining the groups, *limma* package was used to determine the differentially expressed genes in highERK *versus* lowERK HCC samples per dataset. For survival analysis with metabolic genes, a previously reported consistently altered metabolic gene list was used [14]. Upregulated metabolic genes in HCC that were also upregulated in ERK-stratified tumours were named 'highUpMET', whereas those that were low in highERK tumours were named 'lowUpMET' and *vice versa* for the consistently downregulated genes. Subsequently, Kaplan−Meier (KM) survival analysis was performed for tumours that have highERK and the metabolic gene expression pattern indicated in the figures. The data analysis was performed with R software (https://www.r-project.org/), while KM was plotted in GraphPad Prism 8.

2.8. Gene set enrichment analysis (GSEA)

Genes commonly high or low in highERK tumours from GSE14520 ($P<0.05$) and GSE25097 ($P<0.01$) were selected. The average z-score of the genes across the two datasets was used to generate a ranked list of differentially expressed genes in highERK relative to lowERK HCC tumours. Using the ranked list, gene set enrichment analysis was performed with the GSEAPreranked tool (software.broadinstitute.org/GSEA, version 4.0.1).

2.9. Immunohistochemistry

Paraffin-embedded tissues from 15 HCC tumour samples were stained for the expression of Ki67 - Dako (M7240) at 1:70 and pERK - Cell Signalling Technology (9101) at 1:150 following established immunohistochemistry (IHC) protocol. Microscopy images of 5 fields per slide were taken with Zeiss Axio Scope.A1, and staining quantification obtained with ZEN software (blue edition) v2.3.

2.10. Statistical analyses

Results are expressed as mean ± standard deviation (SD) unless stated otherwise. Graphical plots and statistical testing were performed with GraphPad Prism 6−8 (La Jolla, CA, USA). T-test or ANOVA was applied for group comparison where applicable. R software (version 3.5.2) was used for analysing microarray datasets. In general, a *P*-value less than 0.05 was considered statistically significant.

3. Results

3.1. Glutamine deprivation severely impairs metabolism and activates ERK pathway in HCC cells

We previously showed that poorly differentiated HCC cell lines have notable metabolic alterations. These cells express a low level of several genes that encode amino acid pathway enzymes, and are highly dependant on extracellular Gln for proliferation [15]. Here we confirmed their high Gln dependency using an extended panel of 10 cell lines as well as patient-derived primary liver cancer cells (PDLCs) (Fig. 1a, Supplementary Fig. 1a). To understand the link between metabolism and the ERK pathway, we studied the effect of Gln deprivation mainly in a representative poorly-differentiated cell line HLE compared to HUH7 (a well-differentiated cell). These two cells were selected because compared to the others, they have been better characterised at metabolomics, proteomics and signalling levels and found to be largely distinct representative models of HCC molecular features [15]. We found that Gln withdrawal cause a sustained proliferation arrest in HLE cells (Fig. 1b). However, this suppressed growth can be rescued by complete media even after 7 days, indicating that the cells remained viable (Fig. 1b, Supplementary Fig. 1b). Further, oxygen consumption was reduced and can also be rescued by restoring complete media (Supplementary Fig. 1c). In contrast, proliferation arrest and reduced oxygen consumption were not observed in HUH7 cells (Fig. 1b, Supplementary Fig. 1c). Freshly isolated mouse hepatocytes also did not display extracellular Gln dependency (Supplementary Fig. 1d), supporting that Gln dependency is a feature of malignantly transformed cells.

To determine the metabolic changes that accompanied Gln-deprived HLE compared to HUH7 cells, we analysed the cells' intracellular and extracellular metabolite profile following Gln deprivation. In the intracellular compartment, pyruvate and lactate levels were significantly reduced in HLE cells (Fig. 1c), suggesting a reduced glycolytic activity. In addition, the intermediates of the TCA cycle (*e.g.* αKG, malate) were depleted. Also depleted were the intermediates of glutaminolysis/transamination (*e.g.* glutamate, aspartate, alanine) for which Gln is a known biosynthetic substrate. These changes were far less prominent in HUH7 (Fig. 1c), consistent with it being capable of compensatory *de novo* Gln synthesis as previously reported [28]. Of note, the intracellular metabolite profile of HUH7 and HLE cells was largely consistent with, and mirrored, that of the extracellular compartment as assessed under serum-free condition (Fig. 1d). Thus, both intra- and extracellular metabolite profiling confirmed a profound metabolic alteration in Gln-deprived HLE cells. Using isotope tracing, we found that upon Gln deprivation, ^{13}C-glucose labelling of glutaminolysis intermediates (*i.e.* glutamine, glutamate, αKG) was increased in both cell lines. However, consistent with defective metabolism in HLE cells, its glucose-carbon labelling of Gln in the absence of extracellular Gln was only ~27% compared to ~80% in HUH7 cells (Fig. 1e). Glucose-carbon labelling pattern of glutamate and αKG or malate and aspartate was similar in both cells (~46−48%) (Supplementary Fig. 2a), confirming that HLE cells were uniquely inefficient at compensating for extracellular Gln deprivation. Other alterations exclusive to HLE cells, such as increased expression of glucose transporter *SLC2A1* and a high expression of the Warburg effect repressor mitochondrial pyruvate carrier (MPC1) [29] (Supplementary Fig. 2b), supported that HLE cells have a severely compromised glycolysis and other metabolic activities when Gln-deprived.

We performed microarray analysis with the Gln-deprived HLE cells and found a strong downregulation of multiple metabolic pathways (Supplementary Fig. 2c), further confirming that Gln deprivation severely perturbed HLE cell metabolism. These metabolic alterations were accompanied by a strong induction of MAPK/ERK pathway genes (Fig. 1f), including *MAPK12/13, MAP2K2,* and transcriptional regulators *MYC, ATF4, ELK1, DDIT3, MXD1* and *NDRG1* − most of which are often associated with tumourigenic function and previously identified in Gln-deprived HEP3B cells [30]. The MAPK/ERK genes were also similarly expressed in Gln-deprived triple-negative breast cancer cell MDA-MB-231 (Supplementary Fig. 3a), which is a known Gln-reliant cell line [19,23]. Besides triggering the ERK pathway, the metabolic alterations in HLE cells led to the induction of other signalling and inflammatory networks, *e.g.* cytokine-to-receptor interaction, MTORC, tumour necrosis factor alpha and insulin signalling pathways (Fig. 1f, Supplementary Figs. 2c and 6a). Using aminooxyacetate (a pan-transaminase inhibitor) and asparaginase both of which disrupts Gln metabolism [17,22], we validated the expression changes of selected metabolic targets (*GLS*, *FASN*) and ERK pathway genes *AREG*, *MYC*, *MXD1* and found a much stronger response in HLE cells compared to HUH7 cells (Supplementary Fig. 3b). At the protein level, Gln deprivation induced ERK phosphorylation (pERK) in HLE cells by 24 h and this persisted up to 7 days, whereas pERK was induced in HUH7 cells at the later time point (Fig. 1g−h). There was no noticeable change in pERK in mouse hepatocytes (Fig. 1i, 48 h), which as mentioned earlier did not display Gln dependency. Altogether, a severe metabolic impairment as resulted from Gln deprivation in the poorly differentiated cells lead to ERK pathway induction.

3.2. High intracellular serine in the glutamine-deprived state partly influences ERK pathway activity

Consistent with a prior report on HCC cells [31], the serine biosynthesis pathway (SBP) genes, *e.g.* phosphoglycerate dehydrogenase (*PHGDH*) and phosphoserine aminotransferase (*PSAT1*), were prominently upregulated in Gln-deprived HLE cells (Fig. 2a) [31]. The enzymes encoded by these genes mediate the initial steps in *de novo* serine synthesis (Fig. 2b), which raised the possibility that the Gln-deprived cells were actively synthesising serine. This notion, superficially, was supported by our metabolomics data that showed ~2-fold increase in intracellular serine, glycine, and methionine − all three of which are connected via the SBP (Fig. 2b). Further, assessment of independent human HCC tissue- and serum-based metabolomics studies revealed that serine level is elevated in patients samples (Supplementary Table 1), suggesting that serine accumulation has a clinical relevance in HCC. However, in contrast to Gln-deprived cells,

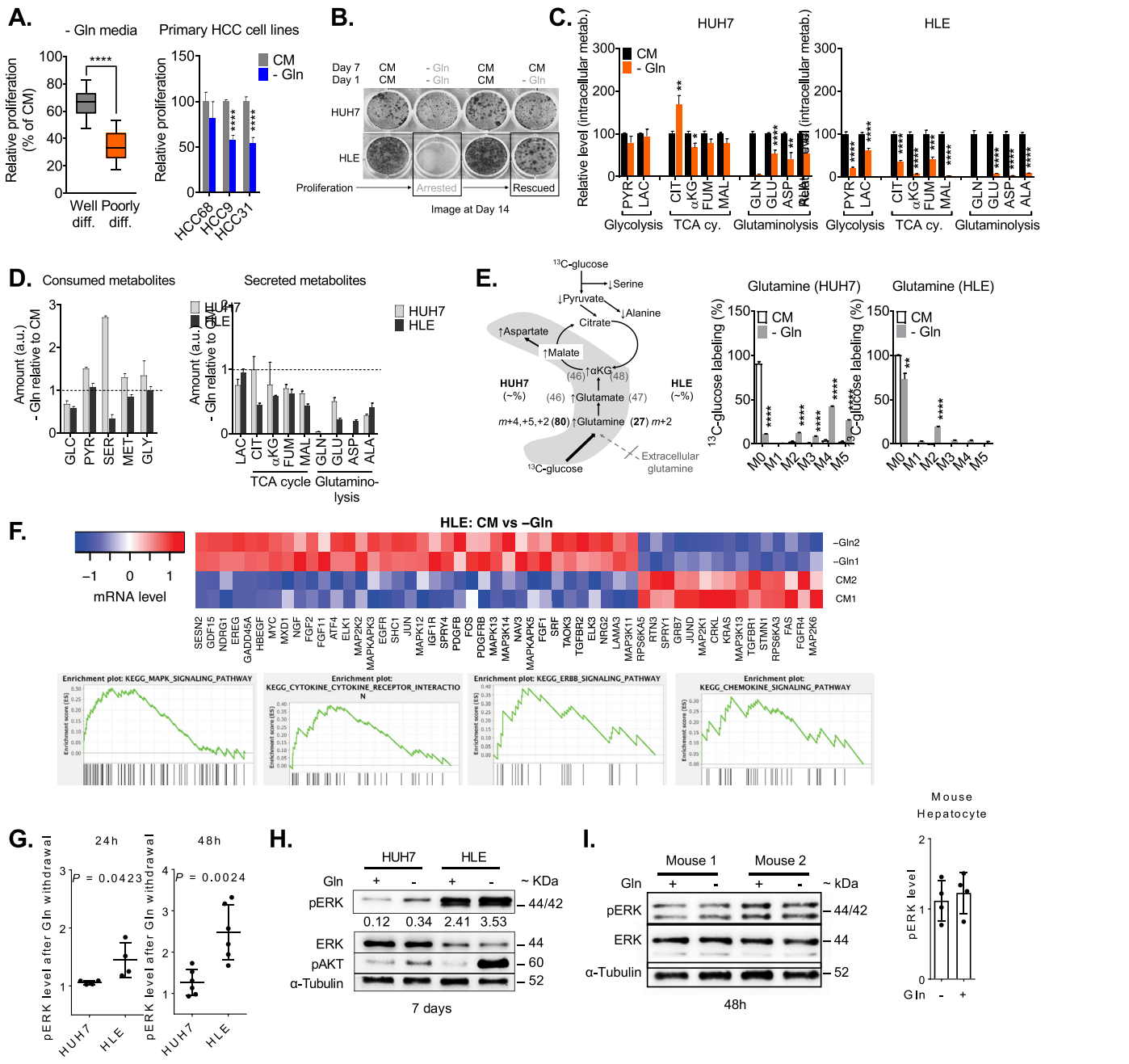

Fig. 1. Severe metabolic alterations in HCC cells activate the ERK pathway. A. MTT proliferation assay of well-differentiated cells compared to poorly differentiated cell lines after 48 h of Gln deprivation. Box plot indicates mean ± S.E.M. of the proliferation data of 5 well-differentiated (HUH7, HEPG2, HEP3B, PLC/PRF/5, HUH1) and 5 poorly differentiated cells (SNU475, SNU398, SNU449, HLE, HLF) in glutamine (Gln)-free relative to complete media (CM). On the right, proliferation of patient-derived primary HCC cells, 72 h. B. Clonogenic assay with or without Gln. Fresh complete media (CM) or glutamine free media (- Gln), was introduced on Day 1 and 7 as indicated. The cells were stained with crystal violet after 14 days culture. C. Intracellular metabolite profile after 24 h culture with or without Gln. Error bars indicate mean ± *S.E.M* of 3 experiments. Cy. Cycle. Pyr – pyruvate, Lac – lactate, Cit – citrate, αKG – alpha ketoglutarate, Fum – fumarate, Mal – malate, Ser – serine, Met – methionine, Gly – glycine, Glu – glutamate, Asp – aspartate, Ala – alanine. D. Extracellular metabolite profile showing the proportion of metabolites consumption or secretion by HUH7 and HLE cells after Gln deprivation in serum-free media. The bars indicate mean ± *S.E.M* of the measured amount at 24, 28, 32 and 48 h after Gln deprivation relative to complete media, which is the baseline indicated with a broken line. Glc – glucose, E. Schematic of ^{13}C-glucose carbon labelling pattern in HUH7 and HLE cells deprived of extracellular Gln as deduced from isotope tracing. Broken line indicates the removal of glutamine from culture media. ↑ - increase, ↓ - decrease. Numbers in bracket indicate % of glucose-derived carbon that labelled the indicated metabolite in the respective cell line. m – the mass shift that contributed the most to the labelling. On the right, ^{13}C-glucose labelling of glutamine in HUH7 and HLE, respectively. F. Heatmap showing the expression pattern of 51 differentially regulated ERK pathway genes ($P<0.05$) in Gln-deprived HLE cells. Underneath, MAPK pathway and other signalling-related pathway enrichment plots. G. Densitometric quantification of pERK level detected in western blots after glutamine deprivation at 24 h and 48 h (quantification from ≥4 experiments). H. Western blot showing pERK induction in HUH7 and HLE cells 7 days after culture in CM or Gln-free media. The western blot run included pAKT (shown). I. Western blot and densitometric quantification of pERK in two mouse hepatocyte isolates (48 h, 2 technical replicates). Error bars represent mean ± SD. Statistical significance: $^{*}P < 0.05$, $^{**}P < 0.01$, $^{***}P < 0.001$, $^{****}P < 0.0001$.

most SBP genes are downregulated in HCC tumours [14]. Thus, we wondered what the connections are between SBP gene induction, high intracellular serine, proliferation arrest and high pERK as seen in HLE cells.

First, we considered that the SBP gene induction is largely indicative of metabolic stress given that glucose deprivation [31] as well as the withdrawal of several other essential amino acids, as observed in published microarrays [32], also induces SBP genes. Thus, we tested

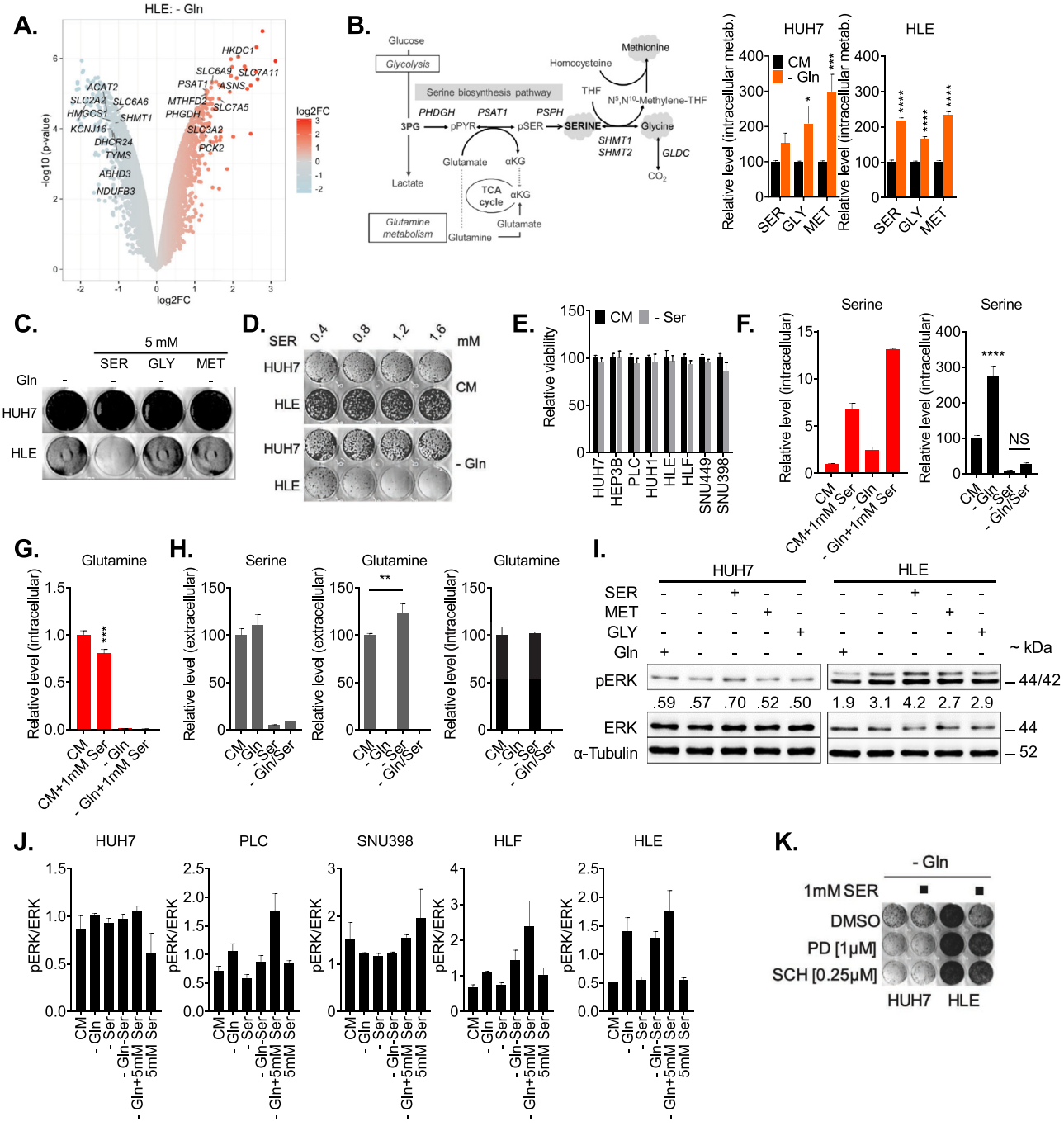

Fig. 2. High intracellular serine contributes to ERK phosphorylation. A. Volcano plot showing the topmost 20 differentially expressed metabolic genes in the microarray of Gln-deprived HLE cells, 24 h. Genes having - log2FC are downregulated; +log2FC are upregulated. B. Schematic depiction of the serine biosynthesis pathway, including the interconnection between serine, glycine and methionine; on the right, intracellular metabolite data showing serine (SER), glycine (GLY) and methionine (MET) levels in Gln-deprived HUH7 and HLE cells. Error bars indicate mean ± S.E.M, representative of 3 experiments. C. Crystal violet staining comparing the effect of 5 mM serine, glycine and methionine on HLE cells, 72 h. Here the cells were seeded at a higher density prior to the metabolite supplementation. Representative of $n>2$ experiments. D. Clonogenic assay showing the selective effect of serine load on HLE cells. Representative of $n>2$ experiments, 72 h. Cell number in − Gln condition was 2x CM condition. E. CellTitre Glo viability assay following serine deprivation in a panel of HCC cell lines, after 48 h. The error bars indicate mean ± SD, $n = 4$. F. Intracellular metabolic profiling showing the level of serine after 24 h culture in the indicated culture media conditions. The error bars indicate mean ± SD, $n = 3$ samples. G. Intracellular metabolic profiling showing the level of glutamine after 24 h in the indicated culture media conditions. The error bars indicate mean ± SD, $n = 3$ samples. H. Extracellular level of serine and glutamine as well as intracellular glutamine after 24 h in the indicated culture media conditions. Error bars indicate mean ± SD, $n = 3$ samples. I. Western blot showing the effect of serine load on pERK levels compared to glycine and methionine, 24 h. Each of the three metabolites were supplemented at 10 mM concentration. J. Western blot densitometric plots of the effect of serine removal or supplementation on pERK levels in 5 HCC cell lines, 24 h. Representative of 2 technical repeat experiments. K. Clonogenic assay showing the protective effect of blocking the ERK pathway on HLE cells supplemented with serine in Gln-deprived state. Cells were treated for 3 days in the indicated conditions, followed by culture in complete media for another 4 days. DMSO − dimethyl sulphoxide (drug solvent).

the involvement of the NRF2-mediated oxidative stress pathway, which has been shown to regulate SBP [33]. *PSAT1* was the most upregulated SBP component upon Gln deprivation (Fig. 2a) and couples Gln metabolism to SBP (Fig. 2b). However, although most NRF2 genes were also upregulated in Gln-deprived HLE cells, the knockdown of NRF2 (*NFE2L2*) did not affect *PSAT1* (Supplementary Fig. 3c). Moreover, stratification of human HCC tumours by ERK signatures (discussed later) showed that *PHGDH*, *PSAT1*, and notable NRF2-

pathway genes (*i.e. NFE2L2, KEAP1, HMOX1, SOD2*) are not high in 'high-ERK' expressing tumours (Supplementary Table 2). We therefore considered the metabolite-level difference *i.e.* high intracellular serine to be more relevant to ERK signalling, given its consistency with the ERK pathway activation *in vitro* and in human HCC.

No prior study has reported that serine, glycine or methionine accumulate under a compromised metabolism. To delineate the implication of such accumulation, we cultured Gln-starved HUH7 and HLE cells with high serine, glycine and methionine (each at 5 mM; equivalent to 12.5–25x normal culture media level). Of the three amino acids, only serine supplementation caused the detachment of the Gln-deprived HLE cells (Fig. 2c). This detrimental effect was evident in HLE cells cultured with ~1 mM (2.5x basal culture media serine) in HLE (Fig. 2d), and in other Gln-reliant cells HEPG2 and HLF cells (Supplementary Fig. 4a), but was not observed in the non-extracellular Gln-reliant cells HUH7 (Fig. 2c–d, Supplementary Fig. 4b) or mouse hepatocytes even at the extremely high serine concentrations (10–20 mM, ~50x normal) (Supplementary Fig. 4c). Serine supplementation in complete media barely suppressed proliferation, albeit having more effect on HLE cells at higher concentration (Supplementary Fig. 4d). Removing serine from media did not affect viability or proliferation of multiple HCC cell lines (Fig. 2e, Supplementary Fig. 4e), together indicating that exogenous serine is dispensable for the HCC cells. Thus, we concluded that a high serine load impedes proliferation only when metabolism is severely impaired.

We next wanted to determine the source of the accumulating serine. As previously reported in breast cancer [34], a possible source of serine is glycolysis through the PHGDH-mediated diversion of 3-phosphoglycerate to serine synthesis (Fig. 2b). However, in both HUH7 and HLE cell lines, isotope tracing experiment showed that ^{13}C-glucose-derived carbon in serine was reduced when Gln is withdrawn (Supplementary Fig. 5a). Since this finding excluded glycolysis as the source of serine in Gln-deprived HLE cells, we considered the extracellular compartment (*i.e.* culture media) as another possible source. Interestingly, extracellular metabolite profiling of serum-free media (shown in Fig. 1d) revealed that overall serine consumption was increased in Gln-deprived HUH7 but reduced in HLE cells. We interpreted this data as implying that HLE cells in a severely compromised metabolic state retain the ability to take up serine but lack the capacity to efficiently metabolise it – hence the accumulation. Consistent with this notion, HLE cells had ~2-fold higher intracellular serine when cultured in Gln-deprived condition compared to complete media when each was supplemented with 1 mM serine (Fig. 2f). On the other hand, intracellular serine was attenuated when serine was withdrawn from culture media (Fig. 2f), supporting that the accumulated serine is from the extracellular compartment.

Serine supplementation marginally reduced intracellular Gln levels, thus partially mimicking Gln deprivation (Fig. 2g). However, although serine withdrawal suppressed Gln consumption (Fig. 2h), most other glutaminolysis metabolites that were depleted by Gln deprivation (*e.g.* glutamate, aspartate and malate) were either elevated or not strongly impacted by serine supplementation or withdrawal (Supplementary Fig. 5b–e). Therefore, we concluded that high intracellular serine is a consequence and not the cause of the severely altered metabolic state, and only partially mimicked Gln withdrawal at the metabolite level.

We then tested whether high serine is linked to the ERK pathway induction. Interestingly, supplementation with serine, but not methionine or glycine, contributed to high pERK in Gln-deprived HLE cells (Fig. 2i), further supporting the selective effect of high serine load. Serine induction of pERK1/2 was further confirmed by ELISA-based phosphoprotein array (Supplementary Fig. 5f), and by immunoblotting in HLF and PLC cell lines, but was not evident in another highly Gln-reliant cell line SNU398 indicating cell-autonomous differences (Fig. 2j, Supplementary Fig. 5 g). Since high pERK increases therapeutic resistance in liver cancer [35,36], we tested whether high serine load impacts HCC cell response to ERK inhibition. We found that when Gln-deprived serine-supplemented HLE cells are co-treated with MEK inhibitors (Fig. 2k), multi-kinase inhibitor Sorafenib and epidermal growth factor receptor inhibitor Erlotinib, the cells became protected from the detachment observed with serine supplementation alone (Supplementary Fig. 5 h). These data provide novel evidence that serine accumulates in a severely impaired metabolic state and contributes to ERK pathway activation as well as kinase inhibitor resistance.

3.3. Blocking the ERK pathway in a severely impaired metabolic state initiates proliferation as a resistance phenotype

Elevated ERK signaling has been observed in various cancer types making it an ideal pathway to target. However, for yet unknown reasons, such intervention also lead to drug resistance [3,5]. Given our observation of high pERK in the background of metabolic alterations and proliferation arrest, we hypothesised that when metabolism is severely compromised, blocking the accompanying pERK could facilitate proliferation as a resistance phenotype. Indeed, a prior study showed that Gln-deprived pluripotent stem cells are more proliferative when cultured with inhibitors of MAPK and GSK3β [37], thus supporting the notion that kinase inhibitors can drive proliferation.

In complete media, Sorafenib, Erlotinib, and MEK/pERK inhibitor (U0126) suppressed the proliferation of HUH7 and HLE cells (Fig. 3a). These inhibitors were less potent in HLE cells (Fig. 3a), which express higher pERK and MAPK genes at basal level [15]. The inhibitors were effective at decreasing pERK level regardless of Gln availability (Fig. 3b). Despite decreasing pERK, the inhibitors had anti-proliferative effect on Gln-deprived HUH7 cells whereas Gln-deprived HLE cells were insensitive to the treatments (Fig. 3c). HLE 'resistance' to pERK inhibition was also evident when U0126 was combined with Asparaginase (Fig. 3c) – an enzyme that mimics Gln deprivation [15,17]. Further, Gln-deprived HLE cells were more proliferative in complete media when pre-treated with pERK inhibitors (U0126, SCH772984, Trametinib and PD0325901) (Fig. 3d). Microarray analysis of the effect of U0126 in Gln-deprived HLE cells confirmed that the inhibitor acts directly on the MAPK/ERK pathway. In addition, U0126 suppressed several signalling and inflammatory components induced by Gln deprivation alone (Fig. 3e, Supplementary Fig. 6a–b). These results reveal that while targeting the MAPK/ERK pathway may be anti-proliferative in unperturbed cellular state, it could enhance proliferation when metabolism is severely compromised. Consistent with the above, treatment with 10058-F4 (an inhibitor of MYC) and the knockdown of the max dimerisation complex 1 *(MXD1),* both of which are downstream of the ERK pathway, also increased the proliferative capacity of Gln-deprived HLE cells (Supplementary Fig. 7a–b). Indeed, an increased pERK did not indicate an increased cell proliferation in the impaired metabolic state. We further confirmed this by stimulating Gln-deprived cells with epidermal growth factor (EGF), which increased pERK level as expected but did not induce HLE cell proliferation (Fig. 3f).

Combination of kinase inhibitors is a clinically tried strategy for overcoming cancer drug resistance. However, contrary to our expectation, the poorly differentiated HCC cell lines are more resistant to the combination of U0126 with Erlotinib and even the well-differentiated cells varied in their response (Fig. 3g, Supplementary Fig. 7c). Noteworthy, while the HCC cells were broadly stratified into well and poorly differentiated subclasses, their mRNA expression of MAP2K1 (MEK1), MAP2K2 (MEK2), MAPK3 (ERK1) and MAPK1 (ERK2) suggest they cluster into at least 4 subsets (Fig. 3h). Resistance to U0126 and Erlotinib combination was most obvious in Gln-deprived HLE and HLF cells, and these two cell lines proliferated more and looked morphologically healthier upon prolonged treatment with the inhibitor combination (Fig. 3i, Supplementary Fig. 7d). When compared to HUH7 cells, Erlotinib combination with the

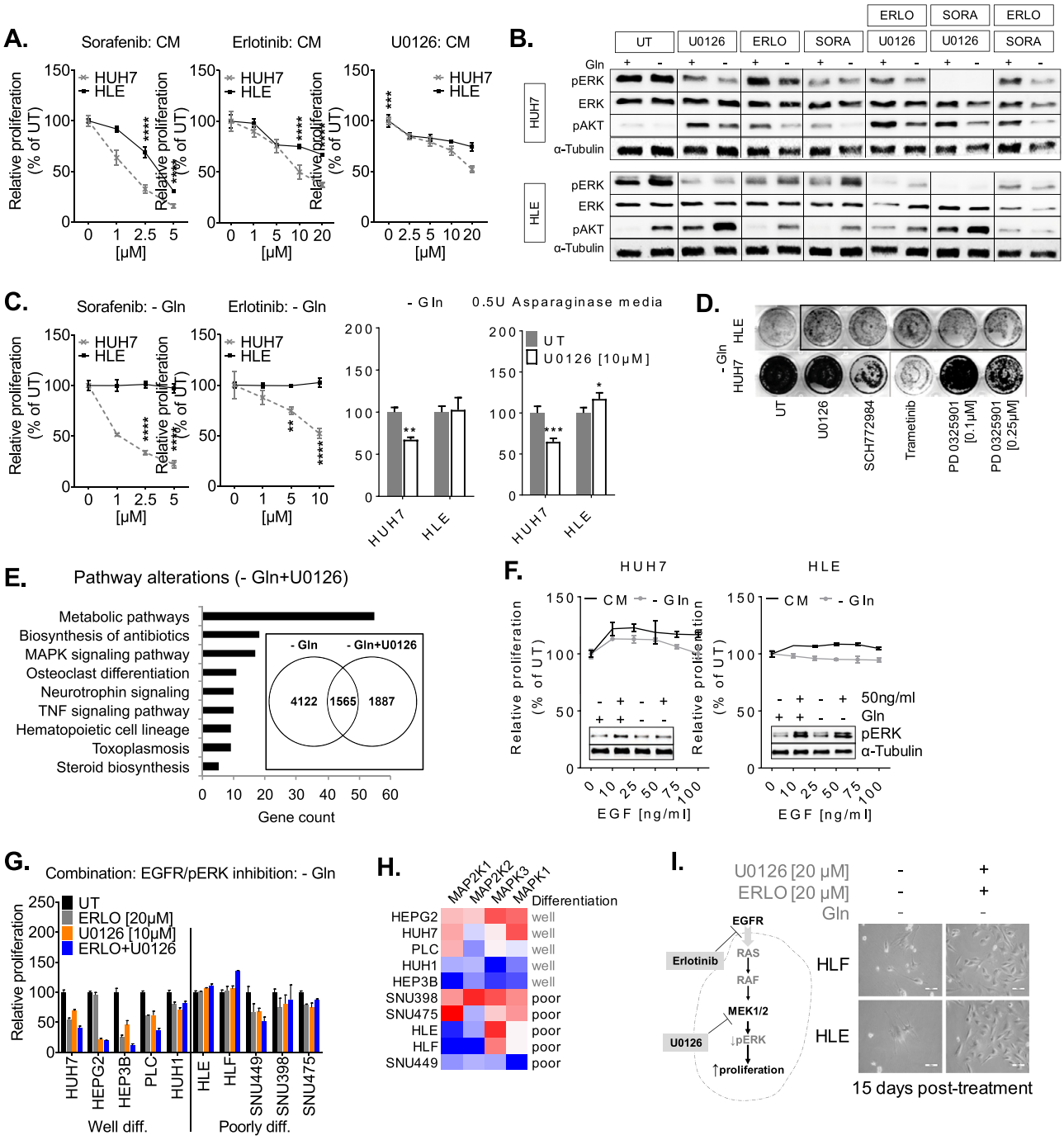

Fig. 3. Blocking the ERK pathway in an impaired metabolic state enables proliferation. A. MTT proliferation assay following treatment of HUH7 and HLE cells with Sorafenib (multi-kinase inhibitor) Erlotinib (EGFR inhibitor), and MEK/pERK inhibitor U0126, in complete medium, 48 h. The asterisks indicate significant p-value compared to the untreated group. B. Western blot analysis of HUH7 and HLE cells treated with the indicated inhibitors, 24 h. C. Proliferation assay, showing the effect of Sorafenib, Erlotinib and U0126 in Gln-deprived media, 48 h. On the right, effect of U0126 in media containing Asparaginase. Asterisks indicate significant p-value compared to the untreated group (UT), which refers to cells cultured in − Gln or in Asparaginase media without U0126. D. Clonogenic assay showing the response of Gln-deprived HUH7 and HLE cells to the indicated MEK inhibitors. The inhibitor concentrations are as follows: U0126 (10 μM), SCH772984 (0.25 μM), Trametinib (0.5 μM). Cells were treated for 4 days, followed by rescue with complete media for 3 days. E. Pathway annotation of 569 genes that were upregulated in Gln-deprived HLE, but suppressed by U0126 treatment [20 μM]. The annotation profile was generated with DAVID (https://david.ncifcrf.gov/tools.jsp). The embedded Venn diagram shows the total number of differentially expressed genes at $P<0.05$. F. Proliferation assay showing the effect of epidermal growth factor (EGF) stimulation, 48 h. The embedded western blots show pERK induction following EGF stimulation, 24 h. G. Proliferation assay showing the effects of Erlotinib, U0126 or a combination of both on the HCC cell lines. H. Heatmap of RT-qPCR results showing the relative mRNA expression of the indicated MAPK/ERK genes in HCC cell lines. Blue − low, Red − high, each gene is scaled relative to the lowest expressing cell line. I. Schematic of ERK pathway inhibition by Erlotinib and U0126, and proliferative effect on the resistant cell lines HLE and HLF. On the right, representative microscopic image showing the appearance of Gln-deprived HLE and HLF cells treated for 15 days with Erlotinib and U0126 combination. Where applicable, statistical significance is $^{*}P < 0.05$, $^{**}P < 0.01$, $^{***}P < 0.001$, $^{****}P < 0.0001$. UT − untreated or drug solvent DMSO where treatment was applied; Number per group = 4 for proliferation assays and plotted relative to UT for either CM or − Gln.

multi-kinase inhibitor Sorafenib also did not affect the Gln-deprived HLE cells (Supplementary Fig. 7e). The kinase inhibitors strongly induced pAKT in both HUH7 and HLE cells (Fig. 3b), which raised the possibility that a compensatory AKT signaling enabled the cell survival in the Gln-deprived state. We ruled out this possibility because treatment with phosphoinositide-3-kinase inhibitor LY294002 itself

facilitated cell proliferation, especially when combined with U0126 (Supplementary Fig. 7f). These results show that when metabolism is severely altered in poorly differentiated HCC cells, high pERK may not indicate higher cell proliferation, and that blocking the ERK pathway can lead to increased cell proliferation.

3.4. Blocking the ERK pathway induces profound metabolic reprogramming that drives resistance

Inhibition of the MAPK pathway following Sorafenib treatment of *ex vivo* HCC tissue was accompanied by altered expression of metabolic pathway enzymes, notably in glycolysis [47]. In line, our microarrays showed that metabolic pathways, alongside MAPK pathway, are the most strongly perturbed in Gln-deprived U0126-treated HLE cells (Fig. 3e). The metabolite changes induced by kinase inhibitors are largely unaddressed in HCC.

We sought to determine the spectrum of metabolite-level changes that accompany MAPK/ERK pathway inhibition, mainly with respect to HLE cells where resistance to the kinase inhibitors occurred upon Gln deprivation. Measurement of glycolytic activity via glucose uptake and lactate secretion showed that U0126 alone (Supplementary Fig. 8a) or in combination with Erlotinib or more potently Sorafenib (Fig. 4a), induced an increase in glycolysis. Consistent with glycolysis being crucial for the kinase-inhibitor resistance, treatment with glycolysis inhibitor 2-deoxy-glucose (2DG) suppressed the residual proliferative activity of Gln-deprived HLE cells (Fig. 4b), and synergised with the combination of Sorafenib and U0126 in eight tested HCC cell lines (Fig. 4b–c). Of note, HUH7 and HLE cells are normally sensitive to 2DG in complete media [15]. Thus, the effect observed with 2DG confirmed that the kinase inhibitors acted via a different mechanism that enable, rather than suppress, metabolic programs that promote cell proliferation.

We compared the intracellular metabolite profile of HUH7 and HLE cells that were treated with U0126 in complete media (*i.e.* where U0126 suppressed proliferation in both cells) or in Gln-deprived media (*i.e.* where HLE cells were insensitive to the anti-proliferative effect of U0126). In complete media, U0126 suppressed most TCA cycle intermediates in both cell lines (Supplementary Fig. 8b). Intermediates of transamination reaction, *i.e.* pyruvate, alanine and aspartate, were also suppressed. U0126 had no tangible effect on the intracellular pool of serine, methionine, glycine, glutamine and glutamate, which were among metabolites earlier identified to be changed by Gln deprivation (Figs. 1 and 2). Noteworthy, U0126 suppressed ^{13}C-glucose-carbon enrichment of serine (Supplementary Fig. 8c), consistent with preventing the diversion of glycolysis intermediates into the SBP pathway. Altogether, under optimal growth conditions, blocking the ERK pathway specifically suppressed the TCA cycle intermediates and downstream components of transamination.

In the Gln-deprived condition, where HLE cell metabolism is severely compromised, U0126 increased the intracellular levels of malate and other TCA cycle intermediates. In addition, components of transamination/glutaminolysis such as glutamine, glutamate, aspartate and alanine were increased (Fig. 4d). Isotope tracing further showed that ^{13}C-glucose-carbon enrichment of notably malate and aspartate is elevated in U0126-treated HLE cells (Fig. 4e). Consistent with a physiologic link between the increase in these metabolites and the ERK inhibitor resistance, culture media supplementation with glutamate, α-ketoglutarate and malate had a rescue effect on the proliferation arrest in Gln-deprived HLE cells (Supplementary Fig. 8d). ERK inhibition suppressed transamination genes (Supplementary Fig. 8e), and reversed metabolic pathway alterations induced by Gln deprivation (Fig. 4f). These data support our proposed model (Fig. 4g) that ERK inhibition enhances cell proliferative capacity when metabolism is severely compromised in a poorly differentiated HCC cell, by inducing glycolysis, the TCA cycle, and other metabolic adaptations.

3.5. Upregulated ERK pathway gene signatures indicate liver tumour metabolic alterations in patients

Our *in vitro* studies showed a strong link between an upregulated ERK pathway and a compromised metabolism. We wanted to know whether such correlation exist in patients. Noteworthy, studies have shown that human HCC tissues often express high pERK, and display profound metabolic alterations at gene, protein and metabolite levels [11,14,38]. To determine if an upregulated ERK pathway correlates with human HCC tumour metabolic alterations, we analysed the expression pattern of ~450 ERK pathway genes in five microarray datasets (consisting of 642 HCC tumour tissue samples in total). We found that the ERK pathway genes are not uniformly upregulated in HCC. Specifically, while most MAPK genes are upregulated (Fig. 5a), growth factors, especially EGF ligands and fibroblast growth factors are either low or not consistently expressed across the cohorts (Supplementary Fig. 9a). We identified 24 ERK gene signatures that have a combined high expression across the five HCC datasets.

Using those 24 ERK gene signatures (Supplementary Fig. 9b), we defined “highERK” and “lowERK” HCC tumours in the two largest datasets in our analysis (Fig. 5b) – each of which contains over 200 tissue samples. In the highERK tumours, the topmost downregulated genes were predominantly metabolic genes (Fig. 5c) and included many poorly understood genes in HCC such as *HPD* (in tyrosine catabolism), *SDS* (in serine catabolism), *CYP4A11* (in xenobiotic metabolism), *FBP1, PCK1* (in gluconeogenesis) and *ALDOB* (in fructose metabolism). Similarly, several metabolic genes were high in highERK tumours, including *HK2, ALDOA, ENO1* (in glycolysis), *TKT* (in pentose phosphate pathway), *ASNS* (in asparagine metabolism), and *ACSL4, SCD, LPCAT1, SQLE* and *FADS1* in cholesterol/lipid metabolism, together suggesting that a high expression of the ERK pathway signatures indicate an altered metabolic profile in human HCC.

While the genes commonly upregulated in highERK clusters from both datasets had high MAPK pathway enrichment as expected, genes commonly downregulated in those tumours were strongly involved in metabolic processes (Fig. 5d), including fatty acid, xenobiotics and amino acid pathways known to be altered in liver and other cancers [39]. Thus, a high ERK pathway signature specifically predicts a severe metabolic alteration in HCC (Fig. 5e), especially for those biochemical pathways involved in physiological liver function. Besides metabolism, we assessed evidence of proliferation in our ERK-stratified datasets given our observation of proliferation arrest along with high pERK *in vitro*. Using a list of known proliferation markers (including TOP2A, MKI67, PCNA, RRM2, MCM2 – 6, CCNB1, CCND1 and CCNE1), we found that most of the proliferation genes were highly expressed in highERK tumours (Fig. 5f), suggesting no overlap with the *in vitro* data with respect to these markers. Nevertheless, immunohistochemical analysis of the proliferation marker Ki67 and pERK in 15 HCC samples yielded variable results between samples, with some samples showing very low pERK staining (Fig. 5g). These data are consistent with a duality in ERK signalling in patients, and suggest a stronger overlap between ERK and metabolism.

We wondered whether highERK genes have a relevant correlation with prognostic outcomes in HCC patients. Using 87 genes that were recently published as predictors of a poor response to Sorafenib [36], we found that ~40% were high in highERK tumours at least in one of the two stratified datasets (Supplementary Fig. 9c). Lastly, we analysed patient survival outcome based on the 24 ERK gene signatures and their accompanying consistently altered metabolic genes in HCC as previously reported [14]. HighERK signatures correlated with poor survival outcome (Fig. 5h). HighERK correlation with poor survival was stronger when the tumours were further stratified using consistently upregulated metabolic genes (Fig. 5i) or downregulated metabolic genes in human HCC tissues (Fig. 5j). Taken together, these data establish a strong link between ERK signalling activation and a dysregulated metabolism in human HCC tumours.

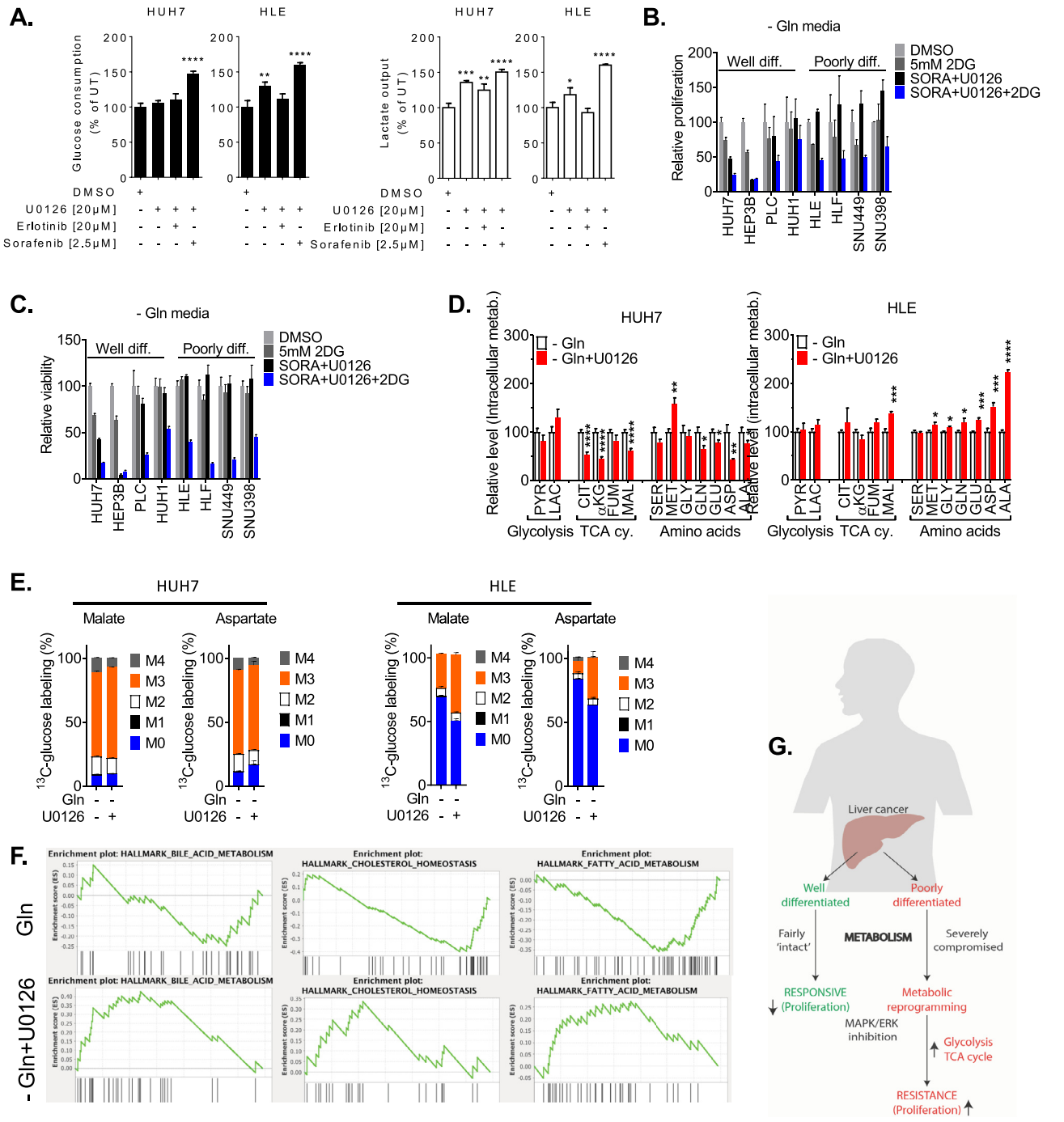

Fig. 4. Blocking the ERK pathway reprograms metabolism. A. Glucose consumption and lactate output after treatment of HUH7 cells (48 h) and HLE cells (24 h) with the indicated inhibitors in the Gln-free media, $n = 3$ per group. B. MTT proliferation assay, 48 h after treatment with glycolysis inhibitor 2-deoxy-glucose, and Sorafenib (2.5 μM)+ U0126 (20 μM) combination; $n = 4$ per group. C. CellTitre Glo viability assay, 48 h after treatment with glycolysis inhibitor 2-deoxy-glucose, and Sorafenib (2.5 μM), U0126 (20 μM) combination; $n = 4$ per group. D. Intracellular metabolite profiling showing the effect of U0126 (20 μM) in Gln-deprived state. Bars indicate mean ± S.E.M. of two experiments. Pyr – pyruvate, Lac – lactate, Cit – citrate, αKG – alpha ketoglutarate, Fum – fumarate, Mal – malate, Ser – serine, Met – methionine, Gly – glycine, Glu – glutamate, Asp – aspartate, Ala – alanine, Cy – cycle, Glutamin. – glutaminolysis. E. Mass isotopologue distribution of ^{13}C-glucose carbon in malate and aspartate in Gln-deprived HUH7 and HLE cells treated with U0126 (20 μM). Bars indicate mean ± S.D, $n = 3$ per group. F. GSEA plots showing metabolic pathways suppressed by Gln deprivation and induced upon the treatment of Gln-deprived HLE cells with U0126. G. Summary of the consequences of inhibiting the ERK pathway in an unperturbed metabolic state of the well-differentiated cell line *versus* in a severely compromised metabolic state of the poorly differentiated HCC cell.

4. Discussion

We provide a new evidence that poorly differentiated HCC cells activate the ERK pathway when metabolism is severely compromised, and propose that this interaction could explain why liver cancer resist kinase inhibitors [7]. We find that at least in two cell lines, phenotypic response to ERK pathway inhibition is governed by metabolic state. To study the link between metabolism and ERK signalling, we took the approach of depriving HCC cells of glutamine. Depriving rapidly proliferating cells of Gln causes a plethora of highly reproducible changes, including the depletion of TCA cycle intermediates, altered expression of transporters/metabolic genes (*e.g. SLC7A11, MPC1, HK2, PC, PSAT1, GLS*), activation of the NRF2-stress pathway, induction of transcription factors (*MYC, MXD1, ATF3/4, DDIT3*), and suppression of proliferation

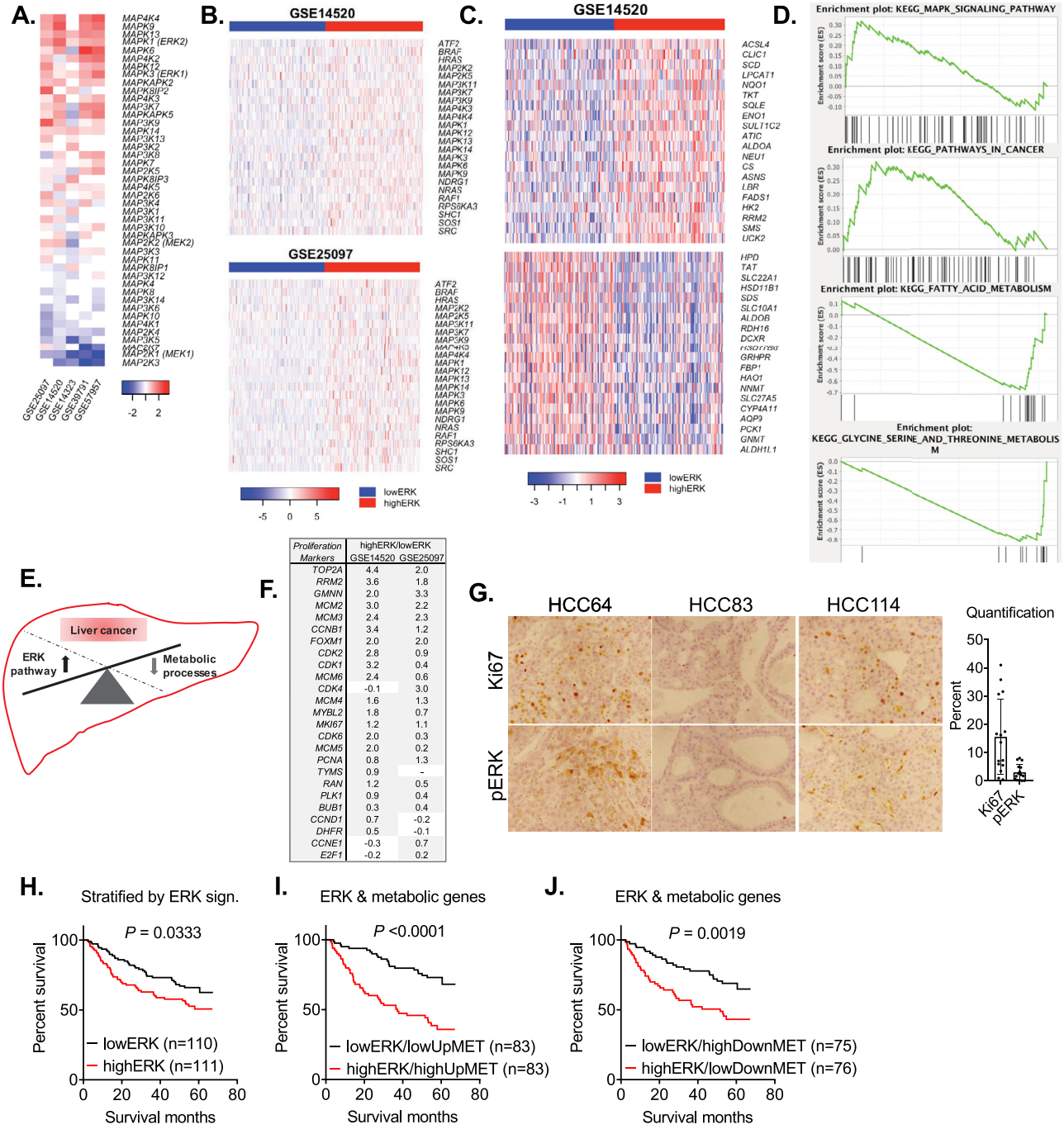

Proliferation Markers	highERK/lowERK GSE14520	GSE25097
TOP2A	4.4	2.0
RRM2	3.6	1.8
GMNN	2.0	3.3
MCM2	3.0	2.2
MCM3	2.4	2.3
CCNB1	3.4	1.2
FOXM1	2.0	2.0
CDK2	2.8	0.9
CDK1	3.2	0.4
MCM6	2.4	0.6
CDK4	-0.1	3.0
MCM4	1.6	1.3
MYBL2	1.8	0.7
MKI67	1.2	1.1
CDK6	2.0	0.3
MCM5	2.0	0.2
PCNA	0.8	1.3
TYMS	0.9	-
RAN	1.2	0.5
PLK1	0.9	0.4
BUB1	0.3	0.4
CCND1	0.7	-0.2
DHFR	0.5	-0.1
CCNE1	-0.3	0.7
E2F1	-0.2	0.2

Fig. 5. High ERK gene signatures indicate altered metabolism in patients tumours. A. Heatmap showing the expression of MAPK genes in 5 human liver cancer microarray datasets. Blue - low expression, red – high expression, white – not significant. Cut-off for significant expression per dataset is $P<0.05$. B. The topmost 24-ERK gene signatures identified from the 5 HCC microarray datasets and used to stratify tumours into highERK and lowERK group in the dataset GSE14520 ($n = 225$ samples) and GSE25097 ($n = 268$ samples). C. Topmost differentially expressed metabolic genes in highERK tumours. Upper panel shows previously defined consistently upregulated genes in HCC that are also high in highERK tumours, while lower panel shows consistently downregulated genes in HCC that are also low in highERK tumours. D. GSEA plot showing the upregulation of MAPK pathway and downregulation of metabolic processes in highERK tumours. Plots were generated using 2607 genes, amongst which 1776 are commonly upregulated in highERK tumours from GSE14520 and GSE25097, whereas 831 are commonly downregulated in highERK tumours in both datasets. E. Schematic representation of a reciprocal balance between ERK pathway activation and metabolic status of HCC. F. Expression profile of proliferation markers in HCC tumours expressing high ERK signatures. Values indicate z-score per dataset. Negative values indicate a downregulation; - indicate not available or statistically significant. G. Representative immunohistochemical stain of Ki67 (proliferation marker encoded by MKI67 gene) and pERK in three patients tissue samples. On the right, a quantification of percentage positive cells from 5 fields per sample from 15 patients. H. Kaplan–Meier overall survival analysis of HCC tissue samples stratified based on the 24-ERK gene signatures. I. Kaplan–Meier overall survival analysis of HCC tissue samples stratified based on the 24-ERK gene signatures and the consistently upregulated metabolic genes in HCC. 'UpMET' or 'DownMET' refers to whether the metabolic genes are those consistently upregulated or downregulated, respectively, in HCC. J. Kaplan–Meier overall survival analysis of HCC tissue samples stratified based on the 24-ERK gene signatures and the consistently downregulated metabolic genes in HCC. The Kaplan–Meier plots were generated with the clinical data from GSE14520. (For interpretation of the references to colour in this figure legend, the reader is referred to the web version of this article.)

[18-22,33,37,40-43]. Several of these molecular changes exist in human tumours when compared to adjacent normal tissues. In addition, they broadly indicate altered cancer metabolism, and have motivated the quest to target Gln metabolism in the clinic [16]. As shown in our study, some of these changes occur in a well-differentiated cell line that can proliferate without extracellular Gln, albeit to a

lesser degree. By comparing a typically extracellular Gln-reliant to a well-differentiated cell, we have unravelled extensive and severe metabolic perturbations that occur mainly in the poorly differentiated cells. We report that under such metabolic impairments, ERK pathway inhibition can accelerate glycolysis and channel glucose-derived carbon towards glutaminolysis intermediates.

Of the metabolic consequences that accompanied Gln deprivation, we were curious about changes in the serine biosynthesis pathway (SBP). The exact function of the SBP is unclear in HCC as well as other cancer types. For example, the SBP was previously identified as a major driver of oncogenesis in breast and colon cancer [34,44,45]. However, in lung cancer the SBP components were found to be heterogeneously expressed and not always functional [33]. In HCC tumours and the poorly differentiated cell lines, most SBP genes are expressed at a low level [14,15]. Upon nutrient starvation, *e.g.* glucose or glutamine deprivation, c-MYC can regulate the SBP in HCC cells [31]. These findings suggest that SBP may be critical or redundant depending on the cell contexts. At least in the context of cell proliferation, c-MYC regulation of SBP seems physiologically counterintuitive since in the Gln-deprived cells MYC is upregulated alongside the SBP genes, whereas proliferation is arrested. Further evidence indicating that the withdrawal of other amino acids or glucose also induces SBP [31,32], suggest that the upregulation of SBP genes following Gln deprivation does not truly reflect serine metabolic activity. Based on our data, we propose that SBP gene induction is highly consistent with proliferation arrest, defective metabolism, and inability to specifically metabolise serine. Consistently, while serine, methionine and glycine accumulate in the absence of Gln, the Gln-reliant HCC cells detach from monolayer only when supplemented with high serine but neither methionine nor glycine. To our knowledge, this is the first evidence showing that poorly differentiated HCC cells need Gln to promote serine metabolism, proliferation, and to maintain a low intracellular serine level. Our experiments in serine-free media provided no compelling evidence of extracellular serine dependency across HCC cell lines. Thus, high intracellular serine as observed in human liver cancer tissues [38] and in non-alcoholic fatty liver disease [46], could be a novel clinically important indicator of severe metabolic impairment. We showed that the high intracellular serine contributed to ERK pathway activation and primed the poorly differentiated cells to kinase inhibitor resistance. Further studies will be required to better understand the clinical role of serine in HCC and the specific portals through which it is internalised.

Another crucial finding of broad clinical implication is the strong correlation between ERK pathway and dysregulated metabolic pathways *in vitro* and in human HCC tissues. Indeed, despite elevated pERK in HCC tumour samples, the reasons for kinase inhibitor resistance is vaguely understood [7]. One possible explanation is that the inhibitors act on unintended targets. For example, the antiproliferative effect of tivantinib as tested in >30 HCC cell lines was reported to be due to its anti-mitotic effect and not due to the expected MET signalling inhibition [51]. Even when acting on the intended targets, a plethora of tumour promoting alterations may occur via currently unknown compensatory mechanisms. Our data suggest that there might be conditions, at least altered cancer metabolism, under which high pERK may not reflect a suppressed cell proliferation. Under such conditions, there might be little or no justification for targeting ERK pathway by itself. Instead, given that tumours resistant to Sorafenib show profound induction of MAPK components and pERK [35,47,48], it is quite probable that high pERK predicts a severely impaired metabolic state and the likelihood of resistance. Consistent with this view, we show that targeting the ERK pathway in the Gln-deprived state induces proliferation and unintended metabolic reprogramming (*e.g.* aerobic glycolysis), which are unfavourable outcomes if occurring in patients. Similar observations have been made in prior studies. For example, Dazert and colleagues observed "a strong enrichment of pathways involved in central carbon metabolism" in a biopsied Sorafenib-treated liver tumour that resisted therapy [47]. In addition, metabolic reprogramming as a driver of resistance has been observed upon NOTCH1 inhibition in T cell acute lymphoblastic leukaemia [49], and with BRAF V600E inhibitor Vemurafenib in melanoma [50]. Thus, our work can facilitate new discoveries on the drivers and predictors of drug resistance in HCC. We also presented 24 consistently upregulated components of the MAPK pathway that predicted the altered metabolic gene profile of HCC patients tumours. Accordingly, we propose the inclusion of metabolic profiling and ERK signatures in the algorithms to stratify HCC patients for kinase inhibitor therapy.

In conclusion, we have found that a severely impaired metabolism can drive ERK pathway activation in a subset of HCC cells. Blocking pERK when metabolism is altered leads to metabolic reprograming and increases the proliferation of such cell lines. While this work is limited by a lack of *in vivo* evidence in experimental models, our analyses of human tumour collectives reveal a solid correlation between high expression of ERK pathway genes and dysregulated metabolic gene networks in HCC tissues. We believe our findings apply more to HCC tumours of poorly differentiated grade, but that tumour heterogeneity may limit the actual subsets even further. We therefore propose that the combination of signatures of impaired metabolism and ERK signalling activation could be an ideal precision medicine strategy to predict HCC patients best suited for kinase inhibitor therapy.

4.1. Ethics approval and consent to participate

Ethics approval or consent to participate were not required for the analysis of the publicly available human HCC datasets. Tissues used for immunohistochemistry were used following patient informed consent and local ethics committee approval (University of Mainz, Germany). Mouse hepatocyte isolation was done according to the approved protocol by Regierungspräsidium Karlsruhe, Germany.

Declaration of competing interest

The authors declare no competing interests with respect to this study.

Acknowledgement

We thank Alexandra Kerner for the assistance with primary mouse hepatocyte isolation. We thank the staff of the Zentrum for Medizinische Forschung, Medical Faculty Mannheim, for the assistance with glucose and lactate assays. We thank Prof. Dr. Iris Behrmann (University of Luxembourg) for critical reading of the manuscript and comments, Prof. Dr. Karsten Hiller (TU Braunschweig, Germany) and other colleagues for discussion of data and assistance.

Funding

SD lab is supported by funds from the DFG (Do373/13−1), BMBF program LiSyM (Grant PTJ-FKZ: 031 L0043) and the Sino-German Cooperation project (GZ126) through the Sino-German Scientific centre. Part of this work was supported through Research grant (*Stiftungsmittel: "Krebs- und Scharlachforschung"*) to ZCN from the Medical Faculty Heidelberg, University of Heidelberg, Germany. CM is supported by a grant from the Deutsche Forschungsgemeinschaft (DFG) (Me4532/1−1). UH is supported by the Federal Ministry of Education and Research (Germany) within the research network Systems Medicine of the Liver (LiSyM) grant 031L0037 and from the Robert-Bosch Foundation (Stuttgart, Germany). The funding bodies did not influence the content of this article.

Author contributions

ZCN: conceptual design of the study, performed experiments, data analyses and wrote the manuscript. NB, PS, LZ, UH: metabolomics

experiments. PH, BB: phosphoprotein array. JL, ZCN: oxygen consumption assay. CD, NG: microarray profiling of glutamine-deprived HLE cells. WP, MH, BD, SP, ZCN, MHW, DC, VC: performed experiments for manuscript revision. JS, SW: provided supervisory support and experimental materials; SD, CM, MPD, CAL, JUM: provided materials, discussed the manuscript; JS, MPE, SD, SW: critical reading of manuscript. SD: corrected manuscript draft and overall supervision of the project.

Data availability and materials sharing

The microarray dataset generated during this study has been deposited in NCBI Gene Expression Omnibus (GEO) under the Accession number GSE123062. Human microarray datasets analysed in this study (*i.e.* GSE14323, GSE25097, GSE14520, GSE39791 and GSE57951) as well as dataset of glutamine-deprived MDA-MB-231 cell (GSE26370) are accessible via NCBI GEO (https://www.ncbi.nlm.nih.gov/geo/). Other data are presented in the manuscript or the supplementary file.

Supplementary materials

Supplementary material associated with this article can be found in the online version at doi:10.1016/j.ebiom.2020.102699.

References

[1] Allemani C, Weir HK, Carreira H, Harewood R, Spika D, Wang XS, et al. Global surveillance of cancer survival 1995-2009: analysis of individual data for 25,676,887 patients from 279 population-based registries in 67 countries (CONCORD-2). Lancet 2015;385(9972):977–1010.

[2] Global Burden of Disease Cancer C, Fitzmaurice C, Dicker D, Pain A, Hamavid H, Moradi-Lakeh M, et al. The global burden of cancer 2013. JAMA Oncol 2015;1(4):505–27.

[3] Caunt CJ, Sale MJ, Smith PD, Cook SJ. MEK1 and MEK2 inhibitors and cancer therapy: the long and winding road. Nat Rev Cancer 2015;15(10):577–92.

[4] Chong CR, Janne PA. The quest to overcome resistance to EGFR-targeted therapies in cancer. Nat Med 2013;19(11):1389–400.

[5] Holohan C, Van Schaeybroeck S, Longley DB, Johnston PG. Cancer drug resistance: an evolving paradigm. Nat Rev Cancer 2013;13(10):714–26.

[6] Bruix J, Qin S, Merle P, Granito A, Huang YH, Bodoky G, et al. Regorafenib for patients with hepatocellular carcinoma who progressed on sorafenib treatment (RESORCE): a randomised, double-blind, placebo-controlled, phase 3 trial. Lancet 2017;389(10064):56–66.

[7] Llovet JM, Hernandez-Gea V. Hepatocellular carcinoma: reasons for phase iii failure and novel perspectives on trial design. Clin Cancer Res 2014;20(8):2072–9.

[8] Zhu AX, Rosmorduc O, Evans TR, Ross PJ, Santoro A, Carrilho FJ, et al. SEARCH: a phase III, randomized, double-blind, placebo-controlled trial of sorafenib plus erlotinib in patients with advanced hepatocellular carcinoma. J Clin Oncol 2015;33(6):559–66.

[9] Pavlova NN, Thompson CB. The emerging hallmarks of cancer metabolism. Cell Metab 2016;23(1):27–47.

[10] Vander Heiden MG, DeBerardinis RJ. Understanding the intersections between metabolism and cancer biology. Cell 2017;168(4):657–69.

[11] Allain C, Angenard G, Clement B, Coulouarn C. Integrative genomic analysis identifies the core transcriptional hallmarks of human hepatocellular carcinoma. Cancer Res 2016;76(21):6374–81.

[12] Cancer Genome Atlas Research Network T. Comprehensive and integrative genomic characterization of hepatocellular carcinoma. Cell 2017;169(7):1327–41 e23.

[13] Kimhofer T, Fye H, Taylor-Robinson S, Thursz M, Holmes E. Proteomic and metabonomic biomarkers for hepatocellular carcinoma: a comprehensive review. Br J Cancer 2015;112(7):1141–56.

[14] Nwosu ZC, Megger DA, Hammad S, Sitek B, Roessler S, Ebert MP, et al. Identification of the consistently altered metabolic targets in human hepatocellular carcinoma. Cell Mol Gastroenterol Hepatol 2017;4(2):303–23 e1.

[15] Nwosu ZC, Battello N, Rothley M, Pioronska W, Sitek B, Ebert MP, et al. Liver cancer cell lines distinctly mimic the metabolic gene expression pattern of the corresponding human tumours. J Exp Clin Cancer Res 2018;37(1):211.

[16] Altman BJ, Stine ZE, Dang CV. From krebs to clinic: glutamine metabolism to cancer therapy. Nat Rev Cancer 2016;16(10):619–34.

[17] Chiu M, Tardito S, Pillozzi S, Arcangeli A, Armento A, Uggeri J, et al. Glutamine depletion by crisantaspase hinders the growth of human hepatocellular carcinoma xenografts. Br J Cancer 2014;111(6):1159–67.

[18] DeBerardinis RJ, Mancuso A, Daikhin E, Nissim I, Yudkoff M, Wehrli S, et al. Beyond aerobic glycolysis: transformed cells can engage in glutamine metabolism that exceeds the requirement for protein and nucleotide synthesis. Proc Natl Acad Sci U S A 2007;104(49):19345–50.

[19] Kung HN, Marks JR, Chi JT. Glutamine synthetase is a genetic determinant of cell type-specific glutamine independence in breast epithelia. PLoS Genet 2011;7(8):e1002229.

[20] Le A, Lane AN, Hamaker M, Bose S, Gouw A, Barbi J, et al. Glucose-independent glutamine metabolism via tca cycling for proliferation and survival in b cells. Cell Metab 2012;15(1):110–21.

[21] Metallo CM, Gameiro PA, Bell EL, Mattaini KR, Yang J, Hiller K, et al. Reductive glutamine metabolism by IDH1 mediates lipogenesis under hypoxia. Nature 2011;481(7381):380–4.

[22] Son J, Lyssiotis CA, Ying H, Wang X, Hua S, Ligorio M, et al. Glutamine supports pancreatic cancer growth through a KRAS-regulated metabolic pathway. Nature 2013;496(7443):101–5.

[23] Timmerman LA, Holton T, Yuneva M, Louie RJ, Padro M, Daemen A, et al. Glutamine sensitivity analysis identifies the xCT antiporter as a common triple-negative breast tumor therapeutic target. Cancer Cell 2013;24(4):450–65.

[24] Castven D, Becker D, Czauderna C, Wilhelm D, Andersen JB, Strand S, et al. Application of patient-derived liver cancer cells for phenotypic characterization and therapeutic target identification. Int J Cancer 2018.

[25] Battello N, Zimmer AD, Goebel C, Dong X, Behrmann I, Haan C, et al. The role of HIF-1 in oncostatin M-dependent metabolic reprogramming of hepatic cells. Cancer Metab 2016;4:3.

[26] Bottger J, Arnold K, Thiel C, Rennert C, Aleithe S, Hofmann U, et al. RNAi in murine hepatocytes: the agony of choice—a study of the influence of lipid-based transfection reagents on hepatocyte metabolism. Arch Toxicol 2015;89(9):1579–88.

[27] Dai M, Wang P, Boyd AD, Kostov G, Athey B, Jones EG, et al. Evolving gene/transcript definitions significantly alter the interpretation of genechip data. Nucleic Acids Res 2005;33(20):e175.

[28] Cheng T, Sudderth J, Yang C, Mullen AR, Jin ES, Mates JM, et al. Pyruvate carboxylase is required for glutamine-independent growth of tumor cells. Proc Natl Acad Sci U S A 2011;108(21):8674–9.

[29] Schell JC, Olson KA, Jiang L, Hawkins AJ, Van Vranken JG, Xie J, et al. A role for the mitochondrial pyruvate carrier as a repressor of the warburg effect and colon cancer cell growth. Mol Cell 2014;56(3):400–13.

[30] Qie S, Liang D, Yin C, Gu W, Meng M, Wang C, et al. Glutamine depletion and glucose depletion trigger growth inhibition via distinctive gene expression reprogramming. Cell Cycle 2012;11(19):3679–90.

[31] Sun L, Song L, Wan Q, Wu G, Li X, Wang Y, et al. cMyc-mediated activation of serine biosynthesis pathway is critical for cancer progression under nutrient deprivation conditions. Cell Res 2015;25(4):429–44.

[32] Tang X, Keenan MM, Wu J, Lin CA, Dubois L, Thompson JW, et al. Comprehensive profiling of amino acid response uncovers unique methionine-deprived response dependent on intact creatine biosynthesis. PLoS Genet 2015;11(4):e1005158.

[33] DeNicola GM, Chen PH, Mullarky E, Sudderth JA, Hu Z, Wu D, et al. NRF2 regulates serine biosynthesis in non-small cell lung cancer. Nat Genet 2015;47(12):1475–81.

[34] Locasale JW, Grassian AR, Melman T, Lyssiotis CA, Mattaini KR, Bass AJ, et al. Phosphoglycerate dehydrogenase diverts glycolytic flux and contributes to oncogenesis. Nat Genet 2011;43(9):869–74.

[35] Negri FV, Dal Bello B, Porta C, Campanini N, Rossi S, Tinelli C, et al. Expression of pERK and VEGFR-2 in advanced hepatocellular carcinoma and resistance to sorafenib treatment. Liver Int 2015;35(8):2001–8.

[36] Pinyol R, Montal R, Bassaganyas L, Sia D, Takayama T, Chau GY, et al. Molecular predictors of prevention of recurrence in hcc with sorafenib as adjuvant treatment and prognostic factors in the phase 3 storm trial. Gut 2019;68(6):1065–75.

[37] Carey BW, Finley LW, Cross JR, Allis CD, Thompson CB. Intracellular alpha-ketoglutarate maintains the pluripotency of embryonic stem cells. Nature 2015;518(7539):413–6.

[38] Huang Q, Tan Y, Yin P, Ye G, Gao P, Lu X, et al. Metabolic characterization of hepatocellular carcinoma using nontargeted tissue metabolomics. Cancer Res 2013;73(16):4992–5002.

[39] Hu J, Locasale JW, Bielas JH, O'Sullivan J, Sheahan K, Cantley LC, et al. Heterogeneity of tumor-induced gene expression changes in the human metabolic network. Nat Biotechnol 2013;31(6):522–9.

[40] Du K, Hyun J, Premont RT, Choi SS, Michelotti GA, Swiderska-Syn M, et al. Hedgehog-YAP signaling pathway regulates glutaminolysis to control activation of hepatic stellate cells. Gastroenterology 2018;154(5):1465–79 e13.

[41] Mullen AR, Wheaton WW, Jin ES, Chen PH, Sullivan LB, Cheng T, et al. Reductive carboxylation supports growth in tumour cells with defective mitochondria. Nature 2011;481(7381):385–8.

[42] Saqcena M, Mukhopadhyay S, Hosny C, Alhamed A, Chatterjee A, Foster DA. Blocking anaplerotic entry of glutamine into the tca cycle sensitizes K-Ras mutant cancer cells to cytotoxic drugs. Oncogene 2015;34(20):2672–80.

[43] Yuneva MO, Fan TW, Allen TD, Higashi RM, Ferraris DV, Tsukamoto T, et al. The metabolic profile of tumors depends on both the responsible genetic lesion and tissue type. Cell Metab 2012;15(2):157–70.

[44] Maddocks ODK, Athineos D, Cheung EC, Lee P, Zhang T, van den Broek NJF, et al. Modulating the therapeutic response of tumours to dietary serine and glycine starvation. Nature 2017;544(7650):372–6.

[45] Possemato R, Marks KM, Shaul YD, Pacold ME, Kim D, Birsoy K, et al. Functional genomics reveal that the serine synthesis pathway is essential in breast cancer. Nature 2011;476(7360):346–50.

[46] Alonso C, Fernandez-Ramos D, Varela-Rey M, Martinez-Arranz I, Navasa N, Van Liempd SM, et al. Metabolomic identification of subtypes of nonalcoholic steatohepatitis. Gastroenterology 2017;152(6):1449–61 e7.

[47] Dazert E, Colombi M, Boldanova T, Moes S, Adametz D, Quagliata L, et al. Quantitative proteomics and phosphoproteomics on serial tumor biopsies from a sorafenib-treated hcc patient. Proc Natl Acad Sci U S A 2016;113(5):1381–6.

[48] Pinyol R, Montal R, Bassaganyas L, Sia D, Takayama T, Chau GY, et al. Molecular predictors of prevention of recurrence in hcc with sorafenib as adjuvant treatment and prognostic factors in the phase 3 storm trial. Gut 2018.
[49] Herranz D, Ambesi-Impiombato A, Sudderth J, Sanchez-Martin M, Belver L, Tosello V, et al. Metabolic reprogramming induces resistance to anti-NOTCH1 therapies in t cell acute lymphoblastic leukemia. Nat Med 2015;21(10):1182–9.
[50] Pan M, Reid MA, Lowman XH, Kulkarni RP, Tran TQ, Liu X, et al. Regional glutamine deficiency in tumours promotes dedifferentiation through inhibition of histone demethylation. Nat Cell Biol 2016;18(10):1090–101.
[51] Rebouissou S, La Bella T, Rekik S, Imbeaud S, Calatayud AL, Rohr-Udilova N, et al. Proliferation Markers Are Associated with MET Expression in Hepatocellular Carcinoma and Predict Tivantinib Sensitivity *In Vitro*. Clin Cancer Res 2017;23(15):4364–75.